Corner Flow Shear Stress, Streamlines and Flow Field

February 15, 2018

1 Analytic Corner Flow Solution for a Rigid Dipping Slab

This notebook presents the calculation of the stress, stream function and velocity generated by a rigid dipping slab moving at a fixed velocity in a semi-infinite isoviscous fluid. The original solution is found in *Introduction to Fluid Dynamics* by Batchelor (1967). In 1969, Dan McKenzie used these equations to model the flow in the mantle driven by a sinking slab in his paper, *On the Causes and Consequences of Plate Tectonics* (McKenzie, 1969). Later, in a paper titled *Angle of Subduction* this analytic model for flow induced by the slab was used to argue that the average dip of slabs is determined by a balance between the weigh of the slab and flow-induced pressure on the slab (Stevenson and Turner, 1977).

Professor Magali I. Billen
Department of Earth and Planetary Sciences
UC Davis
February 15, 2018

1.0.1 Corner Flow Calculation of Constants

It is important to note that the geometry (and thus boundary conditions) used to find the solutions are different in Batchelor (1967) and McKenzie (1969). You can not mix the two, you must choose one geometry and solve for the constants with the appropriate boundary conditions.

I am writing this all out here because I don't want to ever have to re-do this solution by hand (I've done it at least 5 separate times since I was a graduate student... that seems like enough).

I have included the relevant parts of McKenzie (1969) at the end of this notebook. Figure 5 shows the geometry. Note, the mantle wedge is region B and the sub-slab is region A. As this is drawn, the positive x axis is at point c, origin at b and negative x axis at point a. The y-axis is positive downwards. Also, note that the angles are measured in opposite directions (θ_b is counter clockwise, θ_a is clockwise), and θ is also measured in opposite directions in the two different regions(this is important for applying the boundary conditions).

The solution to the flow (conservation of mass and momentum subject to incompressibility) is found by expressing the velocity in terms of a stream function:

$$v = (v_z, \frac{1}{r}\frac{d\psi}{d\theta}, -\frac{d\psi}{dr})$$

Assuming $v_z = 0$ everywhere, then the PDE for the flow, becomes $\nabla^4\psi = 0$. Defining, $\psi = rf(\theta)$ and substituting, the PDE becomes:

$$\frac{d^4 f}{d\theta^4} + 2\frac{d^2 f}{d\theta^2} + f = 0$$

The solution to this PDE is:

$$f(\theta) = A\sin\theta + B\cos\theta + C\theta\sin\theta + D\theta\cos\theta$$

Note that this means that

$$v_r = \frac{df}{d\theta}$$

and

$$v_\theta = -f(\theta)$$

and

$$\frac{df}{d\theta} = A\cos\theta - B\sin\theta + C(\sin\theta + \theta\cos\theta) + D(\cos\theta - \theta\sin\theta)$$

The geometry and boundary conditions are then used to find the constants A, B, C, and D.

For the geometry defined above, the boundary conditions in region A are:
on $\theta = 0$, $v_r = -v$ and $v_\theta = 0$
on $\theta = \theta_a$, $v_r = v$ and $v_\theta = 0$
In region B:
on $\theta = 0$, $v_r = 0$ and $v_\theta = 0$
on $\theta = \theta_b$, $v_r = v$ and $v_\theta = 0$
The constants found using these boundary conditions in region A are:
$A = \frac{-v\theta_a}{\sin\theta_a + \theta_a}$
$B = 0$
$C = \frac{v(1+\cos\theta_a)}{\sin\theta_a + \theta_a}$
$D = \frac{-v\sin\theta_a}{\sin\theta_a + \theta_a}$
and in region B:
$A = \frac{v\theta_b sin\theta_b}{\theta_b^2 - \sin^2\theta_b}$
$B = 0$
$C = \frac{-v(\sin\theta_b - \theta_b\cos\theta_b)}{\theta_b^2 - \sin^2\theta_b}$
$D = \frac{-v\theta_b sin\theta_b}{\theta_b^2 - \sin^2\theta_b}$

These constants have been check against the equations for the stream function given in McKenzie (1969).

The shear stresses are given by
$\sigma_{r\theta} = \frac{2\eta}{r}(C\cos\theta - D\sin\theta)$

I have also checked this against the stress equations in McKenzie (1969). Note, there is a typo in equation 3.17, the term $\cos(\theta_a)$ in the numerator should be $\cos(\theta)$. This is correct in the pressure equations given by Stevenson and Turner (1977). The solution has also been check against the figure in McKenzie (1969).

Finally, the dynamic (flow-induced) pressure in the mantle is just the shear stress ($P = \sigma_{r\theta}$, because $\sigma_{rr} = \sigma_{\theta\theta} = 0$. The pressure is used in the paper by Stevenson and Turner (1977) to estimate the steady-state dip of slabs.

In [86]:
```
import numpy as np
import matplotlib
import matplotlib.pyplot as plt
%matplotlib inline


# Plot on a figure
```

```
plt.rcParams['figure.autolayout'] = False
plt.rcParams['figure.figsize'] = 10, 6
plt.rcParams['axes.labelsize'] = 12
plt.rcParams['axes.titlesize'] = 14
plt.rcParams['font.size'] = 16
plt.rcParams['lines.linewidth'] = 2.0
plt.rcParams['lines.markersize'] = 8
plt.rcParams['legend.fontsize'] = 12

plt.rcParams['text.usetex'] = True
plt.rcParams['font.family'] = "serif"
plt.rcParams['font.serif'] = "cm"
```

In [87]:

```
# Conversion constants
d2r = np.pi/180
sec2yr = 60*60*24*365  # sec to yr
pa2bar = 1e-5

# Parameters that need to be defined for each slab
dip = 45  # degrees
vslabcmyr = 5 # cm/yr
etaslabm = 1e20  # Pa s

vslab = vslabcmyr/100/sec2yr  # m/s

# Set up geometry
thb = dip*d2r # Region B (mantle wedge above slab)
tha = (180-dip)*d2r  # Regiona A (below slab)
print("thb", thb, "tha", tha)

# Set-up Mesh
dx = 2; # km

x = np.arange(-400,200+dx,dx) # km
y = np.arange(0.1,300+dx,dx) # km
[X,Y] = np.meshgrid(x,y)

# Convert to Polar coordinates
R = np.sqrt(X**2 + Y**2)*1000  # meters, same for region A and B
TH = np.arccos(-X/(np.sqrt(X**2 + Y**2))) # for region B with negative X values
THM = np.pi - TH # for region A with positive X values reverse theta.

# Indices defining the two regions
pb = (TH<thb).nonzero()
pa = (TH>=thb).nonzero()

# Initialize matrices
sig = np.zeros(np.shape(R))  # shear stress \sigma_{r\theta}
```

```python
urB = np.zeros(np.shape(R))    # r-components of velocity
uthB = np.zeros(np.shape(R))    # th-components of velocity
urA = np.zeros(np.shape(R))    # r-components of velocity
uthA = np.zeros(np.shape(R))    # th-components of velocity
Ux = np.zeros(np.shape(R))    # x-components of velocity
Uy = np.zeros(np.shape(R))    # y-components of velocity
psiB = np.zeros(np.shape(R))   # stream function in region B
psiA = np.zeros(np.shape(R))    # stream function in region A

# In Region B: mantle wedge
Vcon = vslab/(thb**2 - (np.sin(thb))**2)
A = Vcon*thb*np.sin(thb)
B = 0
C = -Vcon*(np.sin(thb) - thb*np.cos(thb))
D = -Vcon*thb*np.sin(thb)
M = 2*etaslabm

# Shear stress
sig[pb] = M*(C*np.cos(TH[pb])-D*np.sin(TH[pb]))/R[pb]
# Velocity components
urB = A*np.cos(TH) - B*np.sin(TH) + C*(np.sin(TH) + TH*np.cos(TH)) + D*(np.cos(TH)
                                                                       - TH*np.sin(TH)
uthB = -(A*np.sin(TH) + B*np.cos(TH) + C*TH*np.sin(TH) + D*TH*np.cos(TH))
psiB[pb] = -R[pb]*uthB[pb]
# convert to x-y components
Ux[pb] = -urB[pb]*np.cos(TH[pb]) - uthB[pb]*np.sin(TH[pb])
Uy[pb] = -urB[pb]*np.sin(TH[pb]) + uthB[pb]*np.cos(TH[pb])

# In Region A: below the slab
Vcon2 = vslab/(np.sin(tha) + tha)
E = -Vcon2*tha
F = 0
G = Vcon2*(1 + np.cos(tha))
H = -Vcon2*np.sin(tha)

# Shear stress
sig[pa] = M*(G*np.cos(THM[pa])-H*np.sin(THM[pa]))/R[pa]
# Velocity components
urA = E*np.cos(THM) - F*np.sin(THM) + G*(np.sin(THM) + THM*np.cos(THM)) + H*(np.cos(THM
uthA = -(E*np.sin(THM) + F*np.cos(THM) + G*THM*np.sin(THM) + H*THM*np.cos(THM))
psiA[pa] = -R[pa]*uthA[pa]

Ux[pa] = urA[pa]*np.cos(THM[pa]) - uthA[pa]*np.sin(THM[pa])
Uy[pa] = -urA[pa]*np.sin(THM[pa]) - uthA[pa]*np.cos(THM[pa])

Ux = Ux*100*sec2yr
Uy = Uy*100*sec2yr
# Make figure
```

```python
fig = plt.figure()  #(figsize=(12,4), dpi=100)

axes1 = fig.add_axes([0.1, 1.1, 1.4, 0.7]) # left, bottom, width, height (range 0 to 1)
levels = [-200, -100, -50, -25, 25, 50, 100, 200]
cf = axes1.contour(X,Y,sig*pa2bar,levels)
axes1.set_ylim(axes1.get_ylim()[::-1])
axes1.set_xlabel('x (km)')
axes1.set_ylabel('y (km)')
etasmtext = "%4.2g" % etaslabm
vtext = '$V_{slab}$=' + str(vslabcmyr) + ' cm/yr'
etatext = '$\eta_{sm}$=' + etasmtext + ' Pa s, '
diptext = 'dip =' + str(dip)
titletext = "Shear stress: " + vtext + etatext + diptext
axes1.set_title(titletext)
#cb = fig.colorbar(cf,ax=axes1)

axes4 = fig.add_axes([0.1, 0.2, 1.4, 0.7]) # left, bottom, width, height (range 0 to 1)
cf4 = axes4.contour(X,Y,psiB*1e5,[-7, -5, -3, -1])
cf5 = axes4.contour(X,Y,psiA*1e5, [-30, -18, -6])
dd = 8
qv = axes4.quiver(X[::dd,::dd],Y[::dd,::dd],Ux[::dd,::dd],Uy[::dd,::dd],
                  scale = 10, scale_units='inches')
qk = plt.quiverkey(qv, 1.45, 0.93, 5, r'$5 \frac{cm}{yr}$', labelpos='E',
                   coordinates='figure')
axes4.set_ylim(axes4.get_ylim()[::-1])
axes4.set_title("Flow and Streamlines")
```

```
thb 0.7853981633974483 tha 2.356194490192345
```

```
Out[87]: Text(0.5,1,'Flow and Streamlines')
```

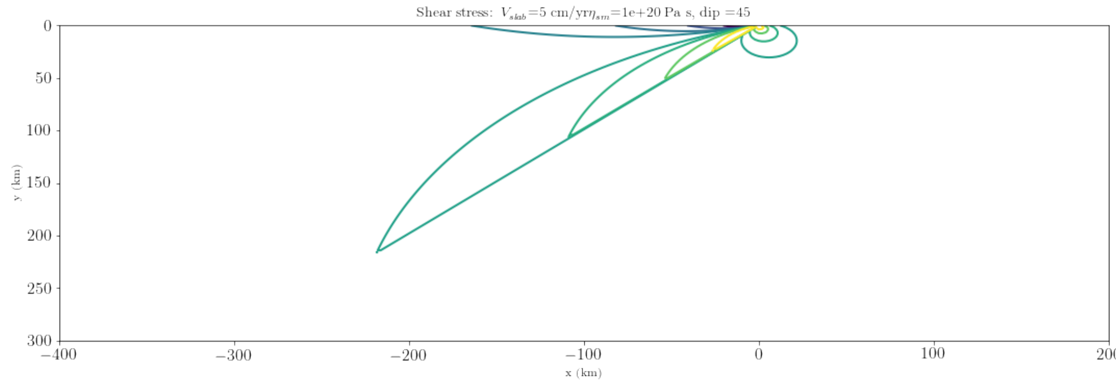
Shear stress: V_{slab}=5 cm/yrη_{sm}=1e+20 Pa s, dip =45
y (km)
x (km)
0
50
100
150
200
250
300
−400
−300
−200
−100
0
100
200

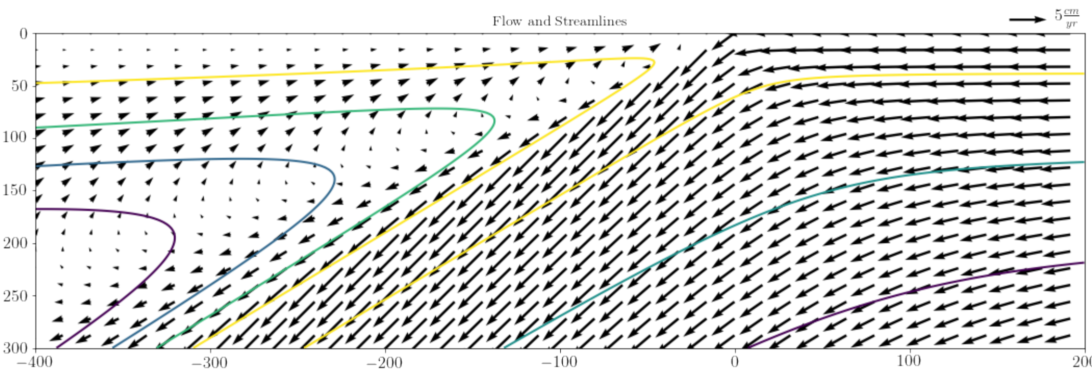
Flow and Streamlines
$5\frac{cm}{yr}$
0
50
100
150
200
250
300
−400
−300
−200
−100
0
100
200

1.0.2 McKenzie, D. P. (GJRAS, 1969), pages 13-15 and figure 7

Subject to these various assumptions the steady state velocity of an incompressible fluid must satisfy:

$$0 = \eta\nabla^2 \mathbf{v} + \rho\nabla U - \nabla P \tag{3.1}$$

$$0 = \nabla . \mathbf{v} \tag{3.2}$$

U is the gravitational potential and P the pressure. The curl of equation (3.1) gives:

$$\nabla^2 \boldsymbol{\omega} = 0 \tag{3.3}$$

where $\boldsymbol{\omega}(= \nabla \times \mathbf{v})$ is the vorticity. Most island arcs are approximately two-dimensional structures, and it is therefore convenient to use cylindrical co-ordinates with the z axis parallel to the arc. Fig. 5 shows a vertical section through an idealized arc, with the motions of the lithosphere and slab represented by the motion of planes. If the co-ordinate axes are fixed to ab, the lithosphere behind the arc, all boundary conditions are simple. Thus $\mathbf{v}$ may be written.

$$\mathbf{v} = \left(v_z, \frac{1}{r}\frac{\partial\psi}{\partial\theta}, -\frac{\partial\psi}{\partial r}\right) \tag{3.4}$$

where ψ is the stream function.

The resulting equations are simple if $v_z = 0$ everywhere, a condition which requires the motion between ab and bc in Fig. 5 to be normal to the arc. This condition is not satisfied by all presently active island arcs (McKenzie & Parker 1967; Le Pichon 1968), and solutions to equation (3.4) can if necessary be obtained if $v_z \neq 0$. It is, however, doubtful if these general solutions would display any features which are not possessed by the special case discussed below. Equation (3.3) then becomes:

$$\nabla^4 \psi = 0 \tag{3.5}$$

Solutions to equation (3.5) are required which satisfy $\mathbf{v} = \mathbf{a}_r \times \text{constant}$, where $\mathbf{a}_r$ is the radial unit vector, at specified values of θ (Fig. 5). Such solutions are easily obtained by substituting (Batchelor 1967).

$$\psi = r\Theta(\theta) \tag{3.6}$$

into equation (3.5) to give:

$$\frac{d^4\Theta}{d\theta^4} + 2\frac{d^2\Theta}{d\theta^2} + \Theta = 0. \tag{3.7}$$

The general solution to equation (3.7) is:

$$\Theta = A\sin\theta + B\cos\theta + C\theta\sin\theta + D\theta\cos\theta \tag{3.8}$$

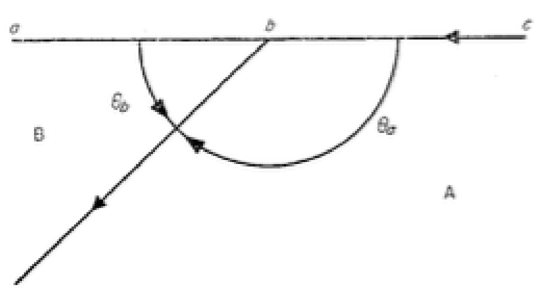

FIG. 5.

where A, B, C and D are constants which must be obtained from the boundary conditions, and are not the same on each side of the island arc. The boundary conditions within region A (Fig. 5) are:

$$\left.\begin{aligned} \mathbf{v} &= -v\mathbf{a}_r \quad \text{on} \quad \theta = 0 \\ \mathbf{v} &= v\mathbf{a}_r \quad \text{on} \quad \theta = \theta_a. \end{aligned}\right\} \tag{3.9}$$

These conditions are satisfied by:

$$\psi = \frac{-rv[(\theta_a-\theta)\sin\theta+\theta\sin(\theta_a-\theta)]}{\theta_a+\sin\theta_a}. \tag{3.10}$$

Similarly the flow within B must satisfy:

$$\left.\begin{aligned} \mathbf{v} &= 0 \quad \text{on} \quad \theta = 0 \\ \mathbf{v} &= v\mathbf{a}_r \quad \text{on} \quad \theta = \theta_b \end{aligned}\right\} \tag{3.11}$$

giving:

$$\psi = \frac{rv[(\theta_b-\theta)\sin\theta_b\sin\theta-\theta_b\theta\sin(\theta_b-\theta)]}{\theta_b^2-\sin^2\theta_b}. \tag{3.12}$$

θ_a in equation (3.10) is measured clockwise from bc in Fig. 5, with bc as zero. θ_b in equation (3.12) is measured anticlockwise from ab as zero. This sign convention simplifies the expressions and is permitted because it is possible to choose a right-handed set of co-ordinate axes in both cases.

Equations (3.9) and (3.11) are not rigorously satisfied in real island arcs because both the surface plates and the sinking slab are finite. This limitation is, however, unlikely to produce important differences in the flow close to the island arc.

The stream lines of constant ψ are easily obtained from equations (3.10) and (3.12) (Fig. 6). Throughout this discussion θ_a and θ_b are chosen to be 135° and 45° respectively. The stream lines demonstrate that the fluid is dragged down with the sinking slab, as indeed would be expected from rather simpler arguments. It is perhaps more surprising that fluid is swept upward in certain parts of region B.

The stresses which the fluid flow produces are also of considerable interest. Since the flow is two-dimensional, the stress tensor $\mathbf{S}$ may be written as:

$$\mathbf{S} = \begin{bmatrix} \sigma'_{rr} & \sigma'_{r\theta} \\ \sigma'_{r\theta} & \sigma'_{\theta\theta} \end{bmatrix} - P\mathbf{1} \tag{3.13}$$

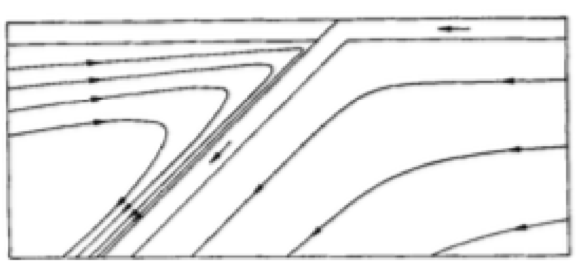

Fig. 6. Stream lines for flow within the mantle. Motion is with respect to the plate behind the island arc, and is driven by the motion of the other plate and of the sinking slab. Thermal convection outside the slab is neglected, and the lithosphere is 50 km thick.

where $\mathbf{I}$ is a 2×2 unit matrix and:

$$\left.\begin{aligned} \sigma'_{rr} &= 2\eta \frac{\partial v_r}{\partial r} \\ \sigma'_{\theta\theta} &= 2\eta\left(\frac{1}{r}\frac{\partial v_\theta}{\partial \theta} + \frac{v_r}{r}\right) \\ \sigma'_{r\theta} &= \eta\left(\frac{1}{r}\frac{\partial v_r}{\partial \theta} + \frac{\partial v_\theta}{\partial r} - \frac{v_\theta}{r}\right). \end{aligned}\right\} \quad (3.14)$$

Equations (3.4) and (3.6) then give:

$$\left.\begin{aligned} \sigma'_{rr} &= \sigma'_{\theta\theta} = 0 \\ \sigma'_{r\theta} &= \frac{\eta}{r}\left(\frac{d^2\Theta}{d\theta^2} + \Theta\right). \end{aligned}\right\} \quad (3.15)$$

Thus:

$$\mathbf{S} + P\mathbf{I} = \begin{bmatrix} 0 & \sigma'_{r\theta} \\ \sigma'_{r\theta} & 0 \end{bmatrix} = \mathbf{S}' \quad (3.16)$$

and forms a tensor $\mathbf{S}'$ without diagonal terms. Thus the greatest shearing stress is exerted parallel to the r = const. and θ = const. surfaces, and is of magnitude $\sigma'_{r\theta}$. Substitution of equations (3.10) and (3.12) into equation (3.15) gives:

this should be theta not theta-a

$$\sigma'_{r\theta} = \frac{2v\eta}{r(\theta_a + \sin\theta_a)}\left[\boxed{\cos\theta_a} + \cos(\theta_a - \theta)\right] \quad (3.17)$$

in A, and:

$$\sigma'_{r\theta} = \frac{2v\eta[\theta_b \cos(\theta_b - \theta) - \sin\theta_b \cos\theta]}{r(\theta_b{}^2 - \sin^2\theta_b)} \quad (3.18)$$

in B. Both equations (3.17) and (3.18) are singular at the origin where $r = 0$. The singularities arise because the spreading lithosphere is required by the boundary conditions (3.9) and (3.11) to bend through an angle θ_b at the origin $r = 0$. Since the radius of curvature of the lithosphere cannot in reality be zero, these singularities are not in practice possible. Thus equations (3.17) and (3.18) are probably good approximations to the stress field except perhaps within 50 km of $r = 0$ axis, and are sufficient for a qualitative discussion. Fig. 7 shows the contours of the shearing stress obtained from equations (3.17) and (3.18) with values for v and η taken from equation (1.2). The half arrows show the direction of the stresses exerted by the fluid on the rigid boundaries. The stresses in region B behind the arc are much greater than those in A. Within B there are two zones of high stress separated by a plane of zero stress. In both zones stresses exceed 100 bars and therefore the viscous constitutional relationship between stress and strain rate does not apply. The occurrence of shallow earthquakes at considerable distances inside the island arc may be related to the shallower of these zones (Hamilton & Gale 1968). Earthquakes also occur within the deeper zone, though their frequency decreases rapidly with depth (Sykes 1966). This observation agrees with the stress distribution in Fig. 7.

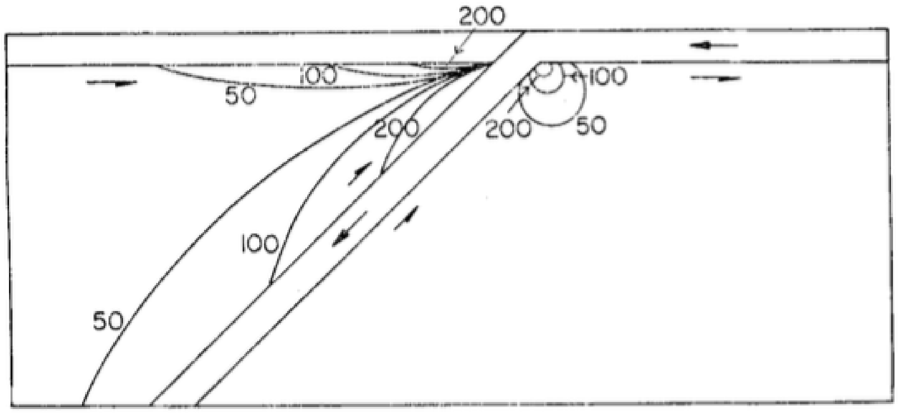

FIG. 7. Shear stresses in bars caused by the flow in Fig. 6. The half arrows show the direction of the forces exerted by the fluid on the plates and slab. The stresses on the plate behind the island arc exceed those on the plate in front. The lithosphere is 50 km thick.

References

Batchelor, G. K., 1967. An Introduction to Fluid Dynamics. Cambridge University Press, Cambridge, UK.

McKenzie, D. P., 1969. Speculations on the consequences and causes of plate motions. Geophys. J. Royal Astron. Soc. 18, 1–32.

Stevenson, D. J., Turner, J. S., 1977. Angle of subduction. Nature 270, 334–336.